J Toxicol Pathol 2022; 35: 255–262

Case Report

Histopathology of acute colchicine intoxication: novel findings and their association with clinical manifestations

Shojiro Ichimata[1], Yukiko Hata[1], Kojiro Hirota[2], and Naoki Nishida[1]

[1] Department of Legal Medicine, Faculty of Medicine, University of Toyama, 2630 Sugitani, Toyama 930-0194, Japan
[2] Department of Intensive Care and Disaster Medicine, Tonami General Hospital, 1-61 Shintomicho, Tonami, Toyama 939-1395, Japan

Abstract: A 32-year-old woman attempted suicide by ingesting Gloriosa bulbs and died approximately 2 days later. Toxicological examination revealed a potentially fatal blood concentration of colchicine (0.096 mg/L). In addition to the increased mitotic figures in the gastrointestinal mucosa, a unique finding for acute colchicine intoxication, pathological examination showed microvesicular lipid droplets in the liver, kidney, heart, and conduction system. Furthermore, central chromatolysis of neurons was observed in the pontine nucleus, medial accessory olivary nucleus, nucleus of the solitary tract, and nucleus ambiguus. Grumose degeneration of the cerebellar dentate nucleus was also evident. These pathological findings may help identify colchicine intoxication, even in the absence of evidence suggesting ingestion during autopsy. Moreover, pathological changes in the heart and central nervous system may be associated with the development of serious complications of acute colchicine intoxication. (DOI: 10.1293/tox.2022-0007; J Toxicol Pathol 2022; 35: 255–262)

Key words: central nervous system, Colchicine, heart, lipid droplets, Reye's syndrome, mitochondria

Colchicine is an alkaloid used to treat different diseases such as acute gout, Mediterranean fever, and Bechet's syndrome[1], typically extracted from *Colchicum autumnale* (autumn crocus, meadow saffron) and *Gloriosa superba* (glory lily)[1]. Accidental ingestion of these toxic species can occasionally occur, as the leaves and roots of *C. autumnale* and *G. superba*, respectively, are similar to those of wild garlic and glutinous yam[2]. Although popular ornamental plants, they have been used to perform suicide[2] and homicide[3].

Following oral ingestion, colchicine is rapidly absorbed and undergoes tissue distribution; the substance then causes severe symptoms that eventually lead to death, depending on the amount ingested[2]. Although some autopsy cases have undergone histopathological examination[4], specific histopathological findings associated with the occurrence of these clinical symptoms in acute colchicine intoxication remain poorly clarified. To date, the mitotic arrest of epithelial cells may be the only unique histopathological finding concerning colchicine intoxication[5].

Herein, we report novel histopathological findings in an autopsy case of acute colchicine intoxication. This study was performed in accordance with the ethical standards established in the 1964 Declaration of Helsinki and approved by the ethics committee of the University of Toyama (I2020006).

A 32-year-old woman with a 6-year history of schizophrenia was admitted to a general hospital for recurrent vomiting, abdominal pain, gait disturbance, and blindness. She informed her family that she had ingested Gloriosa bulbs to commit suicide 36 h earlier. The patient was conscious during emergency transport. However, she was exhausted and appeared pale. Her general condition deteriorated rapidly despite immediate gastric lavage, management with activated charcoal, and intensive supportive treatment. She died of multiple organ failure approximately 2 days after ingesting Gloriosa bulbs. Table 1 shows the laboratory examination results obtained immediately after arrival at the hospital.

A medicolegal autopsy was then performed. The postmortem interval to autopsy performance was 20 h (storage at 4°C). The patient's height was 157 cm and she weighed 57.5 kg. No obvious bulb residues were observed in the gastrointestinal tract. No gross abnormalities leading to death were detected. To qualify and quantify colchicine, blood samples were subjected to colchicine analysis using liquid chromatography with tandem mass spectrometry (LC-MS/MS)[2]. Based on qualitative testing, colchicine was detected in her blood, stomach, intestine, and urine. According to an additional quantitative investigation, her blood colchicine concentration was 0.096 mg/L. Based on a previous report, a concentration of 0.009–0.25 mg/L can be fatal[4].

Received: 12 January 2022, Accepted: 16 February 2022
Published online in J-STAGE: 3 April 2022
*Corresponding author: N Nishida
(e-mail: nishida@med.u-toyama.ac.jp)
(Supplementary material: refer to PMC https://www.ncbi.nlm.nih.gov/pmc/journals/1592/)

Table 1. Laboratory Data upon Admission

CBC			Chemistry					
WBC count	26.6	$\times10^3/\mu L$	TP level	7.0	g/dL	NH_3 level	40	μg/dL
RBC count	5.95	$\times10^6/\mu L$	Alb level	3.5	g/dL	UA level	9.3	mg/dL
Hb level	18.8	g/dL	BUN level	45.4	mg/dL	Na level	146	mEq/L
HCT level	57.2	%	Cre level	4.48	mg/dL	K level	4.1	mEq/L
Plt count	126	$\times10^3/\mu L$	AST level	1,857	U/L	Cl level	95	mEq/L
			ALT level	755	U/L	Ca level	7.3	mg/dL
Coagulation parameters			γ-GT level	98	U/L	Glu level	89	mg/dL
PT	26.1	s	ALP level	2,798	U/L	CRP level	20.17	mg/dL
APTT	71.3	s	LDH level	6,560	U/L	BNP level	825.5	pg/mL
Fibrinogen level	321	mg/dL	AMY level	1,585	U/L	Fer level	21750	ng/mL
DD level	100	μg/mL	CK level	1,699	U/L			

Abbreviations (reference range): Alb: albumin (3.8–5.3 g/dL); ALP: alkaline phosphatase (100–330 U/L); ALT: alanine aminotransferase (8–40 U/L); AMY: amylase (35–120 U/L); APTT: activated partial thromboplastin time (26.1–36.6 s); AST: aspartate aminotransferase (12–31 U/L); BNP: brain natriuretic peptide (0–18.4 pg/mL); BUN: blood urea nitrogen (8.0–22.0 mg/dL); Ca: Calcium (8.4–10.2 mg/dL); CBC: complete blood count; Cl: chrorind (101–108 mEq/L), Cre: creatinine (0.4–0.8 mg/dL); CRP: C-reactive protein (0.0–0.15 mg/dL); DD: D-dimer (0–0.4 μg/mL), Fer: ferritin (5.0–100.0 ng/mL); Glu: glucose (70–109 mg/dL); Hb: hemoglobin (12.0–16.0 g/dL); HCT: hematocrit (34.0%–42.0%); K: potassium (3.5–5.0 mEq/L); LDH: lactate dehydrogenase (110–210 U/L); Na: sodium (135–148 mEq/L), NH3: ammonia (10–70 μg/dL); Plt: platelet (130–320$\times10^3/\mu L$); PT: prothrombin time (10.5–13.5 s); RBC: red blood cell (3.8–4.8$\times10^6/\mu L$); TP: total protein (6.7–8.3 g/dL); UA: uric acid (2.7–5.8 mg/dL); WBC:white blood cell (4.8–9.8$\times10^3/\mu L$); γ-GT: γ-glutamyltransferase (9–49 U/L).

The liver weighed 1,057 g, and the cut surface exhibited a yellow-brown appearance (Fig. 1a). Histopathologically, diffuse microvacuoles were observed in the hepatocytes (Fig. 1b). These vacuoles were positive for Sudan III staining (Fig. 1c) and immunoreactive for adipophilin (Fig. 1d), as confirmed by the presence of lipid droplets (LDs).

The right and left kidneys weighed 154 and 172 g, respectively. The cut surface of the cortex exhibited a white-brown appearance (Fig. 1e). Histopathologically, diffuse microvesicular LDs were observed in the proximal tubules (Fig. 1f–h). These LDs were detected throughout the cytoplasm of the tubules, exhibiting a basal side-predominant distribution.

The heart weighed 268 g, and the cut surface of the ventricles (Fig. 2a, left) exhibited almost the same appearance as the control heart of a 31-year-old woman who had died due to injuries sustained during a traffic accident (Fig. 2a, right). However, the atria exhibited a markedly yellow appearance (Fig. 2a, right). Histopathologically, microvesicular intracytoplasmic LDs were observed in almost half of the left ventricular cardiomyocytes (Fig. 2b–d). Furthermore, atrial cardiomyocytes were diffusely and universally affected. Pyknosis and karyorrhexis foci of both cardiomyocytes and interstitial cells, indicative of apoptosis, were scattered throughout the heart (Fig. 2e). The expression of apoptosis-related immunohistochemical markers, including caspase-3 (Cell Signaling Technology, Danvers, MA, USA, ×400) (Fig. 2f), histone H2AX phosphorylated on Ser 139 (Merck KGAA, Darmstadt, Germany, ×500) (Fig. 2g), and single-stranded deoxyribonucleic acid (IBL, Fujioka, Japan, ×100) (Fig. 2h), were also detected. No evident intracytoplasmic LDs were detected in the sinoatrial or atrioventricular nodes. However, LDs were found in the His bundle and the left and right bundle branches, in addition to the working cardiomyocytes of the basilar ventricular septum (Supplementary Fig. 1). Apoptosis was not observed in the cardiac conduction systems. In addition, this pathology was not observed in skeletal muscle (sternocleidomastoid muscle).

In the lymph nodes and palatine tonsils, the number of apoptotic cells in the germinal center of the lymph follicles was significantly increased (Fig. 3a–d). Additionally, mitotic arrest of epithelial cells was detected in the basal layers of the esophagus (Fig. 3e). The bone marrow was hypocellular and presented moderate depletion of granulocytes and megakaryocytes. However, no significant changes in apoptosis were observed (Fig. 3f). The right and left lungs weighed 925 and 833 g, respectively, and exhibited congestion and diffuse alveolar hemorrhage.

The brain weighed 1,334 g and showed no pathological changes (Fig. 4a). However, histopathological examination revealed central chromatolysis in the neurons of the pontine nucleus, medial accessory olivary nucleus, nucleus of the solitary tract, and nucleus ambiguus in the medulla oblongata (Fig. 4b–e); however, this was not detected in other nuclei of the brain stem (Fig. 4f–h). Additionally, grumose degeneration was observed in the cerebellar dentate nucleus (Fig. 4i). No amyloid precursor protein-positive axonal bulbs were detected.

We showed three novel characteristic histopathological findings that may be critically associated with acute colchicine intoxication: 1) intracytoplasmic microvesicular LD formation in the liver, kidney, and heart; 2) apoptosis of cardiomyocytes; 3) central chromatolysis and grumose degeneration of neurons. Among these three findings, the first was similar to that observed in Reye's syndrome, a condition affecting young children. Moreover, characteristic postmortem findings include cerebral edema and fatty degeneration of the viscera, which are associated with mito-

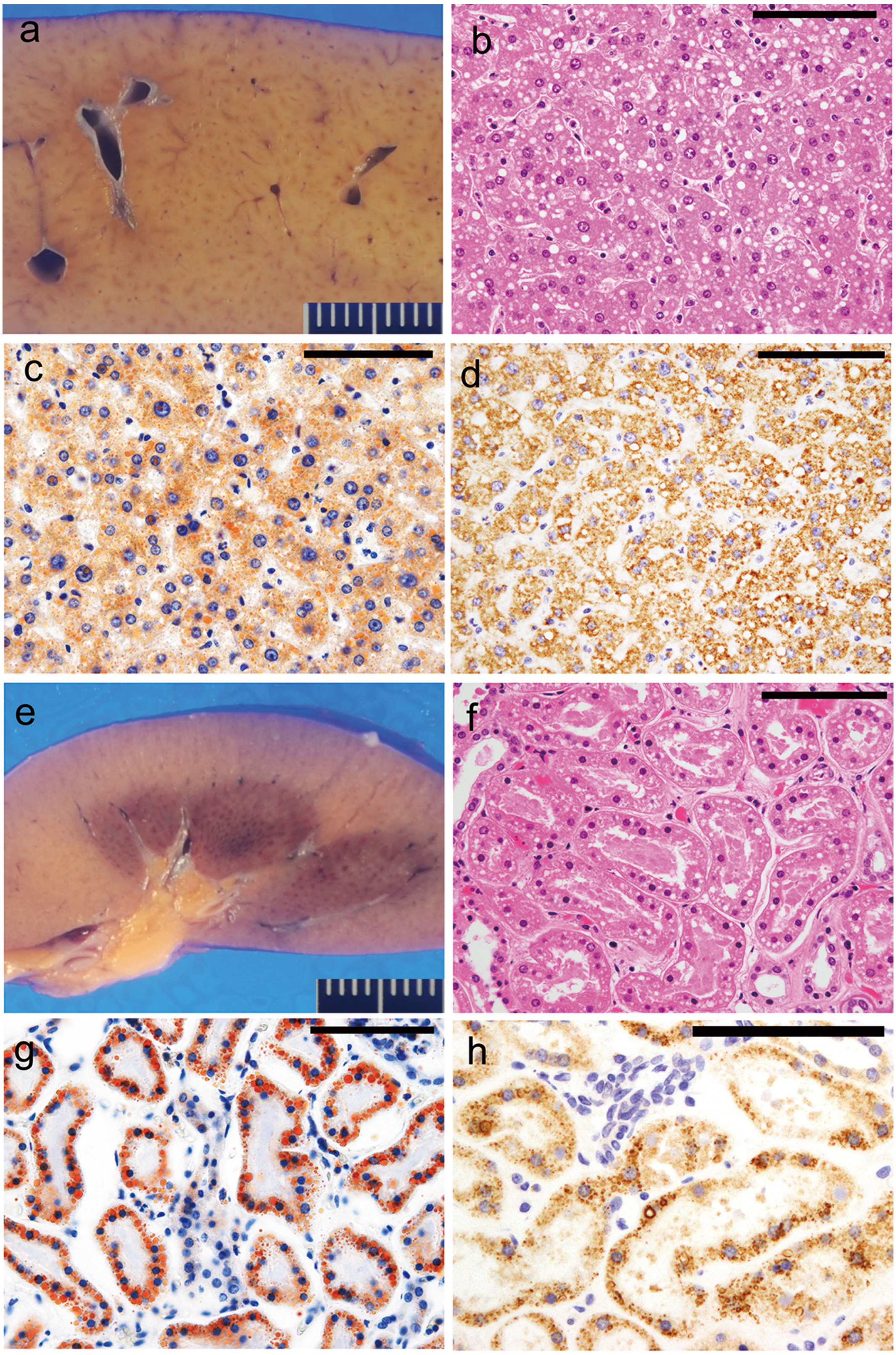

Fig. 1. Macroscopic and histopathological findings in the liver and kidney. (a–d) Liver. (e–h) Kidney. (b, f) Hematoxylin and eosin staining. (c, g) Sudan III staining. (d, h) Immunohistochemistry for adipophilin. (a) The cut surface of the liver exhibits a yellow-brown appearance indicating steatosis. (b–d) Diffuse microvesicular lipid droplets can be observed in the hepatocytes. (e) Cut surface of the kidney. Compared with the medulla, the cortex exhibits a white-brown appearance. (f–h) Diffuse microvesicular lipid droplets can be observed in the proximal tubules. Scale bar=100 μm (b–d, f–h).

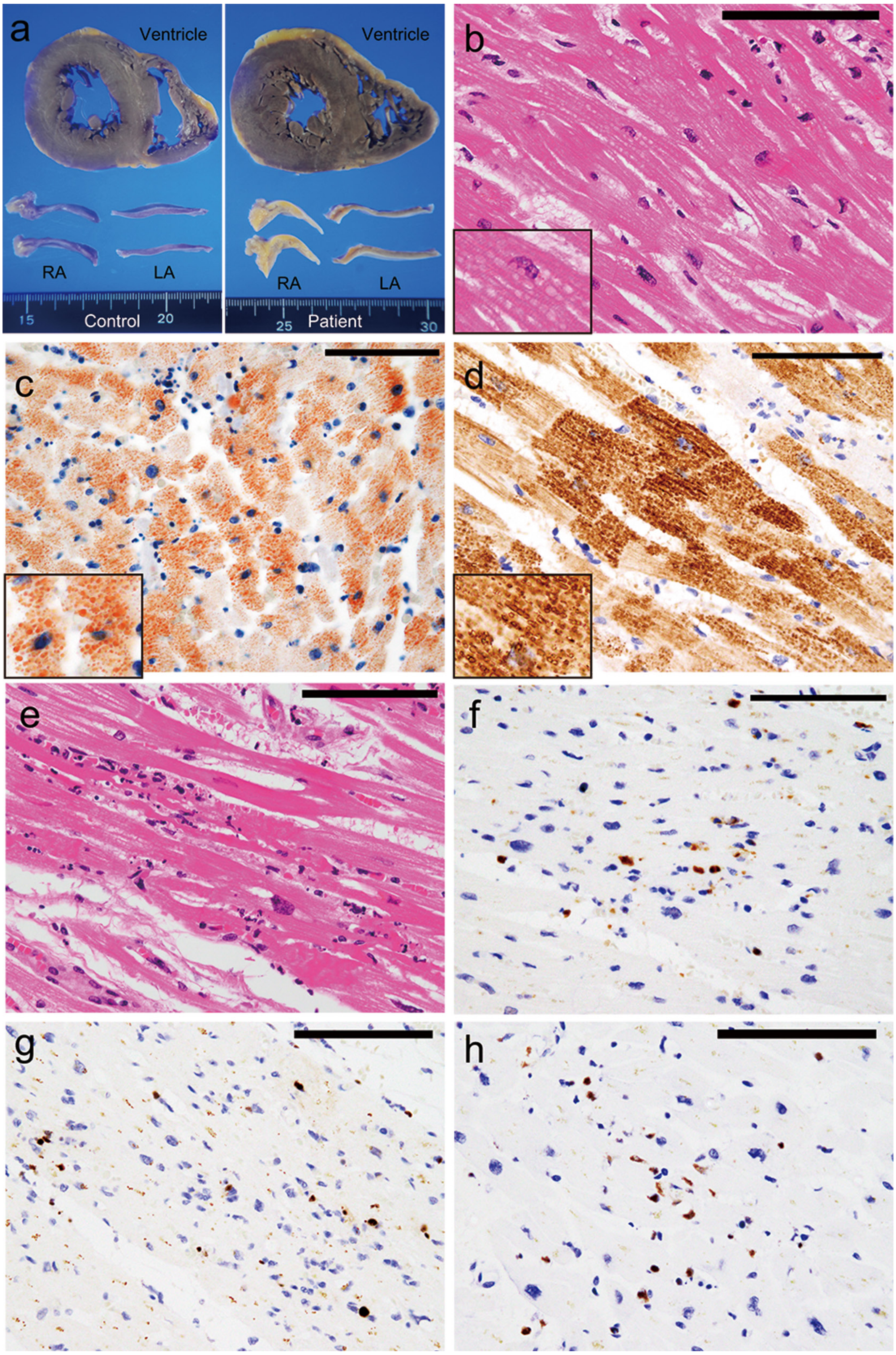

Fig. 2. Macroscopic and histopathological findings in the heart. (b, e) Hematoxylin and eosin staining, (c) Sudan III staining, immunohistochemistry for adipophilin (d), caspase-3 (f), histone H2AX phosphorylated on Ser 139 (g), and single-stranded deoxyribonucleic acid (h). (a) Cut surface of the heart. Compared with the control (left panel), the cut surface of both atria exhibits a significant yellow appearance (right panel). (b–d) Microvesicular lipid droplets can be observed in the myocytes. Inset shows higher magnification views of the droplets. (e) Pyknosis and karyorrhexis foci of the cardiomyocytes and interstitial cells, which are indicative of apoptosis, appear scattered. (f–h) In these foci, immunoreactivities for several apoptosis markers were identified. Scale bar=100 μm (b–h).

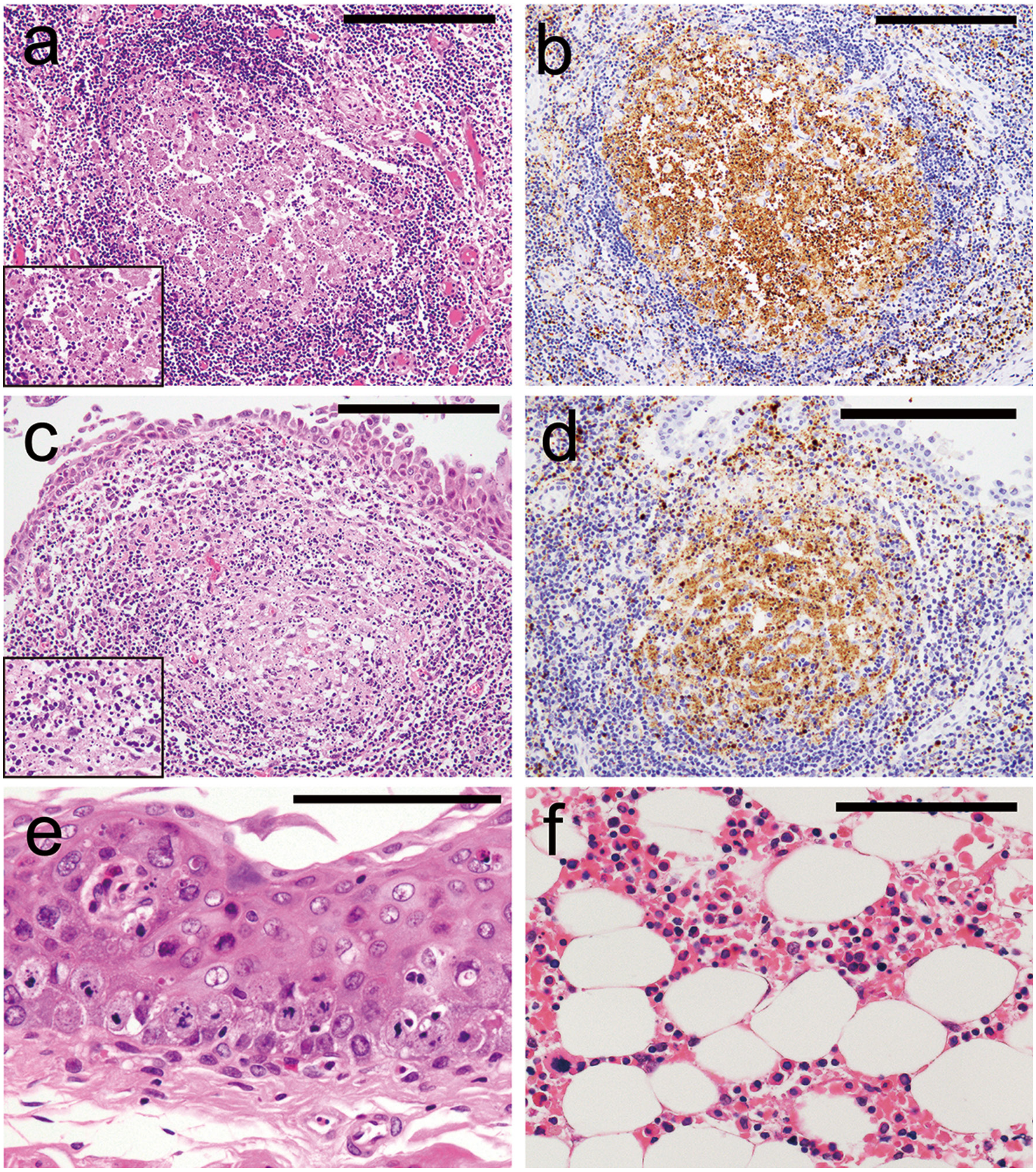

Fig. 3. Histopathological findings in other organs. (a, b) Lymph node, (c, d) palatine tonsil, (e) esophagus, and (f) bone marrow. (a, c, e, f) Hematoxylin and eosin staining, (b, d) immunohistochemistry for caspase-3. (a–d) Evident apoptosis and diffuse immunoreactivity for caspase-3 can be observed in the germinal center of the lymph follicles. Insets in a and c show higher magnification views of apoptotic bodies. (e) Numerous mitotic figures can be identified in the basal layer. (f) Hypocellular bone marrow with moderate depletion of granulocytes and megakaryocytes. Scale bar=200 µm (a–d) and 100 µm (e, f).

chondrial dysfunction[6]. Vacuolar formation, mitochondrial damage of cardiomyocytes, and a high number of caspase-3-positive cells in cardiac interstitial cells have been observed in rats treated with colchicine[7]. Other studies have shown that colchicine induces caspase-3-mediated mitochondrial apoptotic pathways in both normal human cells and cancer cells[8, 9]. Therefore, intracytoplasmic LD formation in cardiomyocytes and apoptosis of both cardiomyocytes and interstitial cells observed in the present case are associated with mitochondrial damage. Intracytoplasmic LD may be a significant disease-specific finding in cases of acute colchicine intoxication. Moreover, the present case demonstrates that lipid staining and immunohistochemistry for adipophilin could help confirm the presence of LDs in these organs. However, we could not conclude whether mitotic arrest of the esophageal mucosa, which was considered a possible unique histological finding[5], was directly associated with colchicine intoxication in the present case. This is

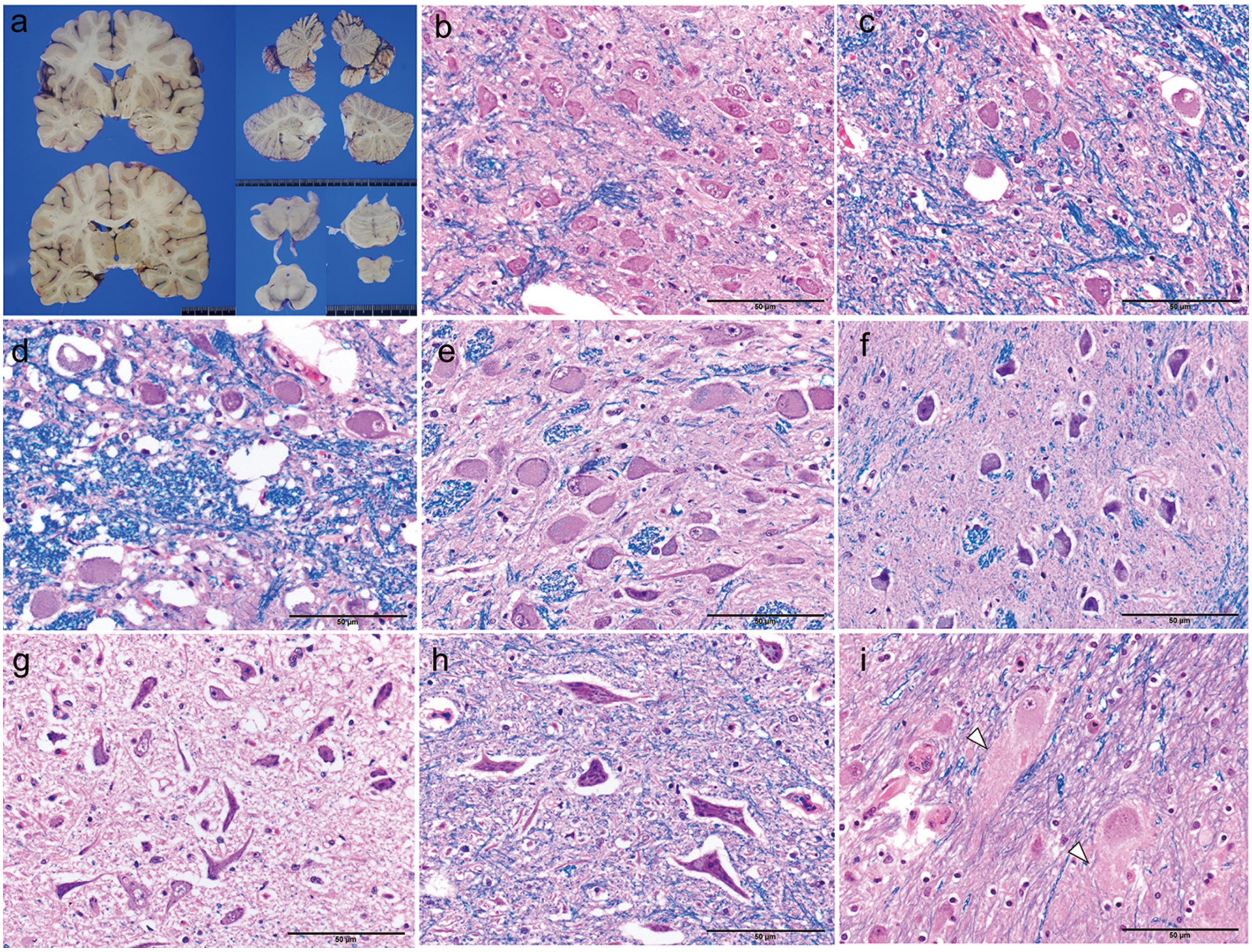

Fig. 4. Macroscopic and histological findings in the brain. (a) Cut surface of the brain (left), cerebellum (upper right), and brain stem (lower right). (b–i) Histological appearance of the brain, Luxol fast blue/hematoxylin-eosin staining. Central chromatolysis can be observed in the pontine nucleus (b), nucleus of the solitary tract (c), nucleus ambiguus (d), and medial accessory olivary nucleus (e). This lesion was absent in the inferior olivary nucleus (f), dorsal vagal nucleus (g), and hypoglossal nucleus (h). (i) Grumose degeneration in the neurons of the cerebellar dentate nucleus (arrowheads). Scale bar=50 µm (b–i).

because gastric acid-induced epithelial cell injury during recurrent vomiting may also cause active regenerative epithelial growth in the esophageal mucosa. Moreover, the laboratory data obtained upon admission did not show significant bone marrow suppression, which may be attributed to the relatively short interval between colchicine administration and hospital admission.

It should be noted that some previous studies have shown that neuromyopathy is a rare side effect of chronic colchicine therapy[10, 11], whereas reports of myopathy are more frequent[10]. Renal failure and co-administration of cytochrome P450-metabolized drugs are known risk factors for myopathy[12]. Vacuolar myopathy with autophagic vacuole accumulation is a significant pathological manifestation of colchicine myopathy in skeletal muscle biopsy[13]. In the present case report, vacuolar myopathy in the skeletal muscle was not observed; therefore, it remains unclear whether the etiology of vacuolar myopathy of the skeletal muscle, revealed in the previous study, and LD in cardiomyocytes, as seen in the present case, represent the same finding. Therefore, further case studies are required.

Three sequential phases have been observed in acute colchicine poisoning: 1) 10–24 h after ingestion (gastrointestinal phase), 2) 24 h to 7 days after ingestion (multiorgan dysfunction phase), and 3) 7–21 days post-ingestion (recovery phase). Patients with acute colchicine intoxication commonly die during the second phase, which is characterized by hemodynamic collapse, cardiac arrhythmias, infection, or hemorrhagic complications[1, 2]. Infectious or hemorrhagic complications are caused by the suppression of cell division in the hematopoietic and lymphatic systems via the pharmacological action of colchicine, which inhibits microtubule polymerization of microtubules[1, 2]. In contrast, data regarding pathological findings associated with hemodynamic collapse and cardiac arrhythmias are limited. Morales *et al.* have shown cardiomyocytic LDs in the distal cardiac conduction system, such as the bundle of His and the left and right branches, in Reye's syndrome. Moreover, the authors revealed that this finding might play a significant role in the outcome of Reye's syndrome, similar to encephalopathy[6]. To the best of our knowledge, the present case report is the first to report the presence of LDs in the bundle of His bundle and the left branch in acute colchicine intoxication. LDs in cardiac conduction fibers may be a crucial pathological substrate of cardiac arrhythmia, possibly associated with death during the early phase of acute colchicine intoxication in the present case.

A previous report has shown acute colchicine poisoning with possible respiratory failure, which was associated with progressive paralysis of the central and/or peripheral nervous system[14]. Central chromatolysis, which was documented in the current case, provides morphological evidence of sublethal cell injury in neurons. Central chromatolysis is a consequence of axonal injury, and chromatolysis can be characterized by reorganization of cell soma and redistribution of Nissl substances to reconstitute injured axons[15]. In an animal study, colchicine was shown to be neurotoxic, as it binds with tau proteins and causes central chromatolysis of neurons after intracerebroventricular injection[16]. Both grumose degeneration in the cerebellar dentate nucleus, which shows degeneration of the axon terminal of Purkinje cells[17], and central chromatolysis are not specific neuropathological findings of colchicine intoxication, given that these features are also observed in other pathological conditions[15]. However, the present study showed that some brainstem nuclei and axon terminals of Purkinje cells might be initially and/or selectively involved in the early phase of acute colchicine intoxication. Cardiac-projecting neurons of the nucleus ambiguus play a critical role in cardiac parasympathetic tone. Their activation elicits bradycardia via acetylcholine release in cardiac ganglia[18]. In addition, a recent study has shown that neurons in the nucleus of the solitary tract are essential for the processing and coordinating respiratory and sympathetic responses to hypoxia[19]. These studies indicate that pathological changes in the circulatory and respiratory centers in the medulla oblongata, as observed in the present case report, may be strongly associated with the prognosis of acute colchicine poisoning.

Herein, we report several novel histopathological findings in an autopsy case of acute colchicine intoxication. Although further case studies should be undertaken, these findings may be crucial not only to prevent overlooking colchicine intoxication during autopsy but to identify its pathophysiology, which is valuable for appropriate treatment.

Disclosure of Potential Conflicts of Interest: The authors have no conflicts of interest to report in connection with this paper.

Acknowledgments: The authors thank Ms. Syuko Matsumori, Ms. Miyuki Maekawa, Ms. Misa Kusaba, and Mr. Osamu Yamamoto for technical assistance. We thank Enago (www.enago.jp) for the English language review.

References

1. Finkelstein Y, Aks SE, Hutson JR, Juurlink DN, Nguyen P, Dubnov-Raz G, Pollak U, Koren G, and Bentur Y. Colchicine poisoning: the dark side of an ancient drug. Clin Toxicol (Phila). **48**: 407–414. 2010. [Medline] [CrossRef]
2. Sakurada M, Yoshioka N, Kuse A, Nakagawa K, Morichika M, Takahashi M, Kondo T, Asano M, and Ueno Y. Rapid identification of Gloriosa superba and Colchicum autumnale by melting curve analysis: application to a suicide case involving massive ingestion of G. superba. Int J Legal Med. **133**: 1065–1073. 2019. [Medline] [CrossRef]
3. Kande Vidanalage CJ, Ekanayeka R, and Wijewardane DK. Case report: a rare case of attempted homicide with Gloriosa superba seeds. BMC Pharmacol Toxicol. **17**: 26. 2016. [Medline] [CrossRef]
4. Klintschar M, Beham-Schmidt C, Radner H, Henning G, and Roll P. Colchicine poisoning by accidental ingestion of meadow saffron (Colchicum autumnale): pathological and medicolegal aspects. Forensic Sci Int. **106**: 191–200. 1999. [Medline] [CrossRef]
5. Gilbert JD, and Byard RW. Epithelial cell mitotic arrest--a useful postmortem histologic marker in cases of possible colchicine toxicity. Forensic Sci Int. **126**: 150–152. 2002. [Medline] [CrossRef]
6. Morales AR, Bourgeois CH, and Chulacharit E. Pathology of the heart in Reye's syndrome (encephalopathy and fatty degeneration of the viscera). Am J Cardiol. **27**: 314–317. 1971. [Medline] [CrossRef]
7. Tochinai R, Suzuki K, Nagata Y, Ando M, Hata C, Komatsu K, Suzuki T, Uchida K, Kado S, Kaneko K, and Kuwahara M. Cardiotoxic changes of colchicine intoxication in rats: electrocardiographic, histopathological and blood chemical analysis. J Toxicol Pathol. **27**: 223–230. 2014. [Medline] [CrossRef]
8. Chen XM, Liu J, Wang T, and Shang J. Colchicine-induced apoptosis in human normal liver L-02 cells by mitochondrial mediated pathways. Toxicol In Vitro. **26**: 649–655. 2012. [Medline] [CrossRef]
9. Zhang T, Chen W, Jiang X, Liu L, Wei K, Du H, Wang H, and Li J. Anticancer effects and underlying mechanism of Colchicine on human gastric cancer cell lines *in vitro* and *in vivo*. Biosci Rep. **39**: BSR20181802. 2019. [Medline] [CrossRef]
10. Kuncl RW, Duncan G, Watson D, Alderson K, Rogawski MA, and Peper M. Colchicine myopathy and neuropathy. N Engl J Med. **316**: 1562–1568. 1987. [Medline] [CrossRef]
11. Tunç A, Gürsoy AE, Güzel V, Gökçal E, and Yıldız GB. Colchicine-induced myoneuropathy with myotonia in a patient with familial Mediterranean fever. Acta Neurol Belg. **120**: 687–688. 2020. [Medline] [CrossRef]
12. Wilbur K, and Makowsky M. Colchicine myotoxicity: case reports and literature review. Pharmacotherapy. **24**: 1784–1792. 2004. [Medline] [CrossRef]
13. Gupta M, Nikolic A, Ng D, Martens K, Ebadi H, Chhibber S, and Pfeffer G. Colchicine myopathy: a case series including muscle MRI and ABCB1 polymorphism data. Front Neurol. **10**: 553. 2019. [Medline] [CrossRef]
14. Gooneratne IK, Weeratunga P, Caldera M, and Gamage R. Toxic encephalopathy due to colchicine—Gloriosa superba poisoning. Pract Neurol. **14**: 357–359. 2014. [Medline] [CrossRef]

15. Vinters HV, and Kleinschmidt-De Masters BK. General pathology of the central nervous system. In: Greenfield's Neuropathology, 9th ed. S Love, H Budka, JW Ironside and A Perry (eds). CRC Press, New York. 1–58. 2015.
16. Sil S, Ghosh R, Sanyal M, Guha D, and Ghosh T. A comparison of neurodegeneration linked with neuroinflammation in different brain areas of rats after intracerebroventricular colchicine injection. J Immunotoxicol. **13**: 181–190. 2016. [Medline] [CrossRef]
17. Ishizawa K, Lin WL, Tiseo P, Honer WG, Davies P, and Dickson DW. A qualitative and quantitative study of grumose degeneration in progressive supranuclear palsy. J Neuropathol Exp Neurol. **59**: 513–524. 2000. [Medline] [CrossRef]
18. Gherghina FL, Tica AA, Deliu E, Abood ME, Brailoiu GC, and Brailoiu E. Effects of VPAC1 activation in nucleus ambiguus neurons. Brain Res. **1657**: 297–303. 2017. [Medline] [CrossRef]
19. Zoccal DB, Furuya WI, Bassi M, Colombari DS, and Colombari E. The nucleus of the solitary tract and the coordination of respiratory and sympathetic activities. Front Physiol. **5**: 238. 2014. [Medline] [CrossRef]